Reactions of 1-Naphthyl Radicals with Acetylene. Single-Pulse Shock Tube Experiments and Quantum Chemical Calculations. Differences and Similarities in the Reaction with Ethylene

Assa Lifshitz,* Carmen Tamburu, and Faina Dubnikova

Institute of Chemistry, The Hebrew University of Jerusalem, Jerusalem 91904, Israel

Received: June 10, 2009; Revised Manuscript Received: August 11, 2009

The reactions of 1-naphthyl radicals with acetylene were studied behind reflected shock waves in a single-pulse shock tube, covering the temperature range 950−1200 K at overall densities behind the reflected shocks of $\sim 2.5 \times 10^{-5}$ mol/cm^3. 1-Iodonaphthalene served as the source for 1-naphthyl radicals. The [acetylene]/[1-iodonaphthalene] ratio in all of the experiments was ~100 to channel the free radicals into reactions with acetylene rather than iodonaphthalene. Only two major products resulting from the reactions of 1-naphthyl radicals with acetylene and with hydrogen atoms were found in the post shock samples. They were acenaphthylene and naphthalene. Some low molecular weight aliphatic products at rather low concentrations, resulting from an attack of various free radicals on acetylene, were also found in the shocked samples. In view of the relatively low temperatures employed in the present experiments, the unimolecular decomposition rate of acetylene is negligible. One potential energy surface describes the production of acenaphthylene and 1-naphthyl acetylene, although the latter was not found experimentally due to the high barrier (calculated) required for its production. Using quantum chemical methods, the rate constants for three unimolecular elementary steps on the surface were calculated using transition state theory. A kinetics scheme containing 16 elementary steps was constructed, and computer modeling was performed. An excellent agreement between the experimental yields of the two major products and the calculated yields was obtained. Differences and similarities in the potential energy surfaces of 1-naphthyl radical + acetylene and those of ethylene are presented, and the kinetics mechanisms are discussed.

I. Introduction

The reaction of aryl radicals with unsaturated aliphatic hydrocarbons is one of the reaction channels that leads to the production of polycyclic aromatic hydrocarbons (PAH). This is particularly true when acetylene and its derivatives are concerned.[1−14] The same holds for the unsaturated aliphatic hydrocarbon radicals reacting with aromatic compounds.

We have recently published a detailed investigation of naphthyl radical reactions with ethylene including potential energy surface calculations and single-pulse shock tube experiments of reaction product distribution.[15] Although some quantum chemical calculations on the phenyl radical + ethylene reaction were reported,[12−14] we were not aware of any quantum chemical calculations or experimental results on the reactions of the naphthyl radical with ethylene.

The reactions of various aryl radicals with acetylene have been studied quite extensively in the past, particularly when phenyl radicals are concerned.[1−11] Both theoretical and experimental results have been reported. When the reactions of naphthyl radicals with acetylene are concerned, very detailed theoretical calculations[1,2,8] have been performed (quantum chemical, RRKM, etc.), but as far as we are aware, no experimental results that can support these calculations have been published.

A very comprehensive and thorough computational investigation on the reactions of phenyl and naphthyl radicals with acetylene was performed by Richter et al.[1] The authors have calculated a large number of potential energy surfaces leading to a variety of intermediates and stable products, resulting from addition of acetylene to the aryl radical with and without H-atom ejection. They also calculated rate constants for various reactant → product systems based on the pathways on the potential energy surfaces. Whereas for the phenyl + acetylene system the results of the theoretical calculations could be compared to existing experimental results,[10,12,13] there were no available experimental data on the naphthyl + acetylene system.

In this article, we present experimental single-pulse shock tube results of product formation and quantum chemical calculations in the system of 1-naphthyl radicals and acetylene, where the 1-naphthyl radicals are obtained from the dissociation of 1-iodonaphthalene. Although the potential energy surface for naphthyl + acetylene has been calculated by Richter et al.,[1] for the sake of comparison with ethylene we decided to repeat these calculations with the same level of theory and basis set that has been used with naphthyl + ethylene. We also compose a kinetics scheme and perform computer simulation based on the reaction pathways and the elementary steps on the calculated surface with additional, mainly bimolecular, reactions. We then compare the results of the calculations to the single-pulse shock tube data. Also, differences and similarities in the potential energy surfaces of 1-naphthyl radical + acetylene and those of ethylene are presented, and the kinetics mechanisms are discussed.

II. Experimental Section

1. Apparatus. The reactions of 1-naphthyl radicals with acetylene were studied behind reflected shock waves in a pressurized driver, 52 mm i.d., single-pulse shock tube. The shock tube had a 4 m long driven section divided in the middle by a 52 mm i.d. ball valve. The driver section had a variable

* Corresponding author. E-mail: assa@vms.huji.ac.il.

10.1021/jp905448g CCC: $40.75
Published on Web 09/08/2009

length up to a maximum of 2.7 m and could be varied in small steps to obtain the best cooling conditions. A 36 L dump tank was connected to the driven section at a 45° angle toward the driver near the diaphragm holder to prevent reflection of transmitted shocks. The driven section was separated from the driver by "Mylar" polyester films (BROWNELL-ELECTRO) of thicknesses ranging between 1 and 2 mil depending upon the desired shock strength.

The shock tube, the reaction mixture storage bulbs, the gas handling manifold, and the transfer tubes were all maintained at 170 ± 2 °C with a heating system containing 15 independent computer-controlled heating elements. Reaction dwell times behind the reflected waves were approximately 2.0 ± 0.1 ms, and cooling rates were ~5 × 10^5 K/s.

Prior to performing an experiment, the tube and its gas handling system were pumped down to ~3 × 10^{-5} Torr. The reaction mixtures were introduced into the driven section between the ball valve and the end plate, and pure argon into the section between the diaphragm and the valve, including the dump tank. After each experiment, two gas samples were taken for analysis. One sample was transferred from the tube through a heated injection system to a Hewlett-Packard model 5890A gas chromatograph operating with a flame ionization detector (FID), using a 15 m × 0.53 mm HP-1 megabore column, coated with methyl silicon gum. This analysis provided the concentrations of the heavy aromatics. The second sample, which gave the conversion of the chemical thermometers (will be mentioned later) and the concentration of the low molecular weight acetylene decomposition products, was transferred from the shock tube via 100 cm^3 glass bulbs to a Carlo-Erba Vega series 2, model 6300 gas chromatograph using a 2 m Porapak-N column with a flame ionization detector.

2. Temperature Determination. Reflected shock temperatures were determined from the conversion of two standard reactions, the reactants of which were added in small quantities (0.01%) to the reaction mixtures to serve as chemical thermometers. Over the temperature range 900−1050 K, the reflected shock temperatures were determined from the extent of the total isomerization of cyclopropanecarbonitrile to cis and trans crotonitrile and 3-butenonitrile,[16] and over the temperature range 1050−1200 K, from the extent of decomposition of 1,1,1-trifluoroethane to 1,1-difluoroethylene + HF.[17]

The reaction rate constants used were:

1. cyclopropanecarbonitrile → *c*-$CH_3CH{=}CHCN$, *t*-$CH_3CH{=}CHCN$, and $CH_2{=}CHCH_2CN$,

$$k_{uni} = 3.82 \times 10^{14} \exp(-57\,840/RT)\ s^{-1}$$

2. $CF_3{-}CH_3 \rightarrow CF_2{=}CH_2 + HF$, $k_{uni} = 3.23 \times 10^{14} \exp(-72\,540/RT)\ s^{-1}$

where R is expressed in units of cal/(K.mole).

Reflected shock temperatures T_5 were calculated from the relation:

$$T_5 = -(E/R)/\left[\ln\left\{-\frac{1}{A \times t}\ln(1-\chi)\right\}\right]$$

where t is the reaction dwell time, A and E are the pre-exponential factors and the activation energies of the chemical thermometer reactions, and χ is the extent of reaction defined as: $\chi = [\text{reactant}]_t/([\text{reactant}]_t + [\text{product(s)}]_t)$.

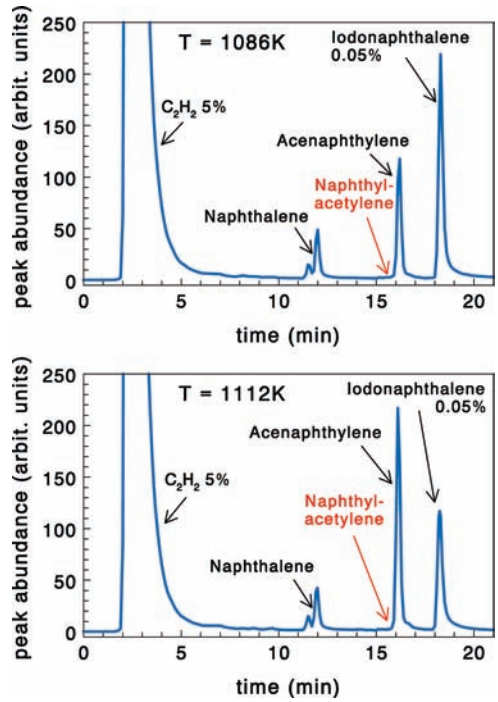

Figure 1. Typical chromatograms of reaction mixtures containing 0.05% 1-iodonaphthalene and 5% acetylene, shock-heated to 1086 and 1112 K. As can be seen, 1-naphthylacethylene is not formed at both temperatures.

Density ratios were calculated from the measured incident shock velocities using the three conservation equations and the ideal gas equation of state.

3. Materials and Analysis. Reaction mixtures containing 0.05% iodonaphthalene, 5% acetylene, and 0.01% of each one of the two chemical thermometer reactants diluted in argon were prepared in 12 L glass bulbs and stored at 170 ± 2 °C and 700 Torr. Both the bulbs and the line were pumped down to approximately 3 × 10^{-5} Torr before the preparation of the mixtures. 1-Iodonaphthalene served as the source of naphthyl radicals as the C−I bond dissociation energy in 1-iodonaphthalene is by some 46 kcal/mol lower than that of the C−H bond in naphthalene (66 vs 112 kcal/mol) and can thus produce naphthyl radicals at much lower temperatures.[18] The reason for the high [acetylene]/[1-iodonaphthalene] ratio (~100) comes to channel all of the radicals, particularly the naphthyl radicals, to reactions with acetylene rather than 1-iodonaphthalene.

1-Iodonaphthalene was obtained from Aldrich Chemical Co. and had a purity of ~97%. None of the major products, acenaphthylene and naphthalene, were found in the unshocked samples. The argon used was Matheson ultra high purity grade, listed as 99.9995%, and the helium driver gas was Matheson pure grade, listed as 99.999%. All materials were used without further purification.

Typical chromatograms of shock-heated samples originally containing 0.05% iodonaphthalene, 5% acetylene, and 0.01% of each of the two chemical thermometer reactants shock-heated to 1086 and 1112 K are shown in Figure 1. As can be seen in these two chromatograms, naphthyl acetylene is not among the reaction products.

4. Data Reduction. The concentrations of 1-iodonaphthalene and the two aromatic ring products in the shocked samples $C_5(\text{pr}_i)$ were calculated from their GC peak areas using the

following set of relations that are based on two fused aromatic rings balance:

$$C_5(\mathrm{pr}_i) = A(\mathrm{pr}_i)/S(\mathrm{pr}_i) \times \{C_5(\mathrm{reactant})_0/A(\mathrm{reactant})_0\} \quad \text{(I)}$$

where

$$C_5(\mathrm{reactant})_0 = \{p_1 \times \%(\mathrm{reactant}) \times \rho_5/\rho_1\}/100RT_1 \quad \text{(II)}$$

and

$$A(\mathrm{reactant})_0 = A(\mathrm{reactant})_t + \sum A(\mathrm{pr}_i)_t/S(\mathrm{pr}_i) \quad \text{(III)}$$

$C_5(\mathrm{reactant})_0$ is the concentration of 1-iodonaphthalene behind the reflected shock prior to reaction, and $A(\mathrm{reactant})_0$ is its calculated GC peak area prior to reaction (eq III), where $A(\mathrm{pr}_i)_t$ is the peak area of a product i in the shocked sample, and $S(\mathrm{pr}_i)$ is its sensitivity relative to that of the reactant, ρ_5/ρ_1 is the compression behind the reflected shock, and T_1 is the initial temperature, 443 K in the present series of experiments.

The low molecular weight aliphatic products that are coming from the acetylene and the very low concentrations of some single ring aromatics such as phenyl acetylene and of indene were not taken into account in these calculations. In view of their low concentration, only those of naphthalene and acenaphthylene were considered.

The GC sensitivities of the products relative to the reactant were determined from standard mixtures. GC peak areas were recorded and evaluated using the "Chromatography Station for Windows − CSW 1.7" software, produced by Data Apex Ltd., 1998, The Czech Republic. They were transferred after each analysis to a PC for data reduction and graphical presentation.

III. Experimental Results

Some 50 tests were run with reaction mixtures containing 0.05% 1-iodonaphthalene, 5% acetylene, and the two chemical thermometers diluted in argon, covering the temperature range 900−1200 K. Densities behind the reflected shocks were ~2.5 × 10^{-5} mol/cm^3 corresponding to p_5 = ~1400−1850 Torr depending upon the temperature. Two major products resulting from the reactions of the system containing 1-iodonaphthalene and acetylene, acenaphthylene and naphthalene, were found in the shocked samples. Figure 2 shows the data points of the two, above-mentioned, products and of the reactant as product yield (in mole percent) versus temperature. The reflected shock temperatures of the low temperature data points (shown in red) were calculated from the isomerization rate of c-C_3H_5CN, and the high temperature data (shown in blue) were calculated from the extent of decomposition of 1,1,1-trifluoroethane. The + signs on the lines are the calculated points based on the computer modeling, and the lines are the best fits to these points.

IV. Quantum Chemical and Rate Constant Calculations

1. Quantum Chemical Calculations. We used the Becke three-parameter hybrid method[19] with the Lee−Yang−Parr correlation functional approximation with unrestricted open shell wave functions (uB3LYP)[20] and the Dunning correlation consistent polarized valence double ζ(cc-pVDZ) basis set.[21] Structure optimization of the reactants and products was done using the Berny geometry optimization algorithm.[22] For determining transition state structures, we used the combined synchronous transit-guided quasi-Newton (STQN) method.[23] Higher level (CI) calculations were done using these structures.

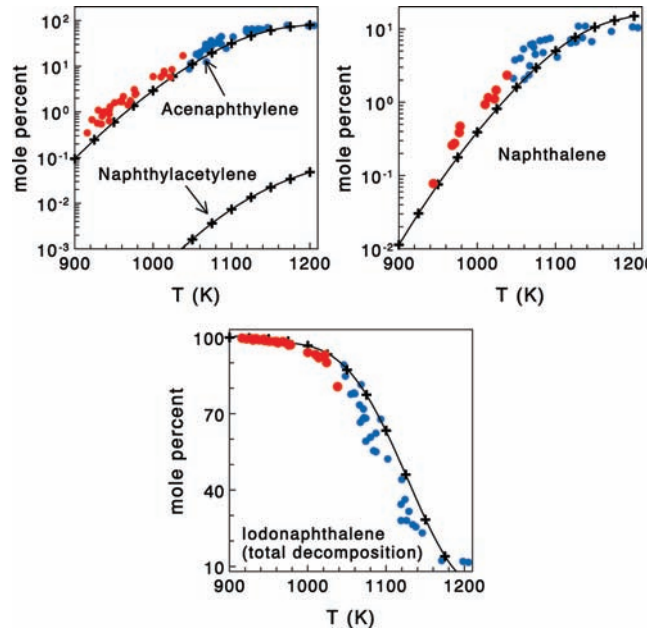

Figure 2. Yields of the acenaphthylene and naphthalene are shown as mole percent vs temperature on a semilog scale. Also shown is the total decomposition of 1-iodonaphthalene. The reflected shock temperatures of the points shown in red were calculated using the extent of the total isomerization of cyclopropane carbonitrile, and the ones in blue are from the extent of decomposition of 1,1,1-trifluoroethene. The black points (+) are the calculated yields, and the lines are the best fit to these points. As can be seen, the agreement is very good.

All of the calculations were performed without symmetry restrictions. Vibrational analyses were done at the same level of theory to characterize the optimized structures as local minima or transition states. Calculated vibrational frequencies and entropies (at uB3LYP level) were used to evaluate preexponential factors of the reactions under consideration. All of the calculated frequencies, the zero-point energies, and the thermal energies are of harmonic oscillators. The calculations of the intrinsic reaction coordinate (IRC), to check whether the transition states under consideration connect the expected reactants and products, were done at the B3LYP level of theory with the same basis set as was used for the stationary point optimization. These calculations were done on all of the transition states.

Each optimized uB3LYP structure was recalculated at a single point with coupled cluster method, including both single and double substitutions with triple excitations uCCSD(T). The uCCSD(T) calculations were performed with the frozen core approximation. All of the reported relative energies include zero-point energy correction (ZPE). The DFT and CCSD(T) computations were carried out using the Gaussian 03 program package.[24]

2. Rate Constant Calculations. To evaluate first-order rate constants from the quantum chemical calculations, the relation:

$$k_\infty = \sigma(kT/h) \exp(\Delta S^{\#}/R) \exp(-\Delta H^{\#}/RT) \quad (1)$$

was used,[25,26] where h is Planck's constant, k is Boltzmann's factor, σ is the degeneracy of the reaction coordinate, and $\Delta H^{\#}$ and $\Delta S^{\#}$ are the temperature-dependent enthalpy and entropy

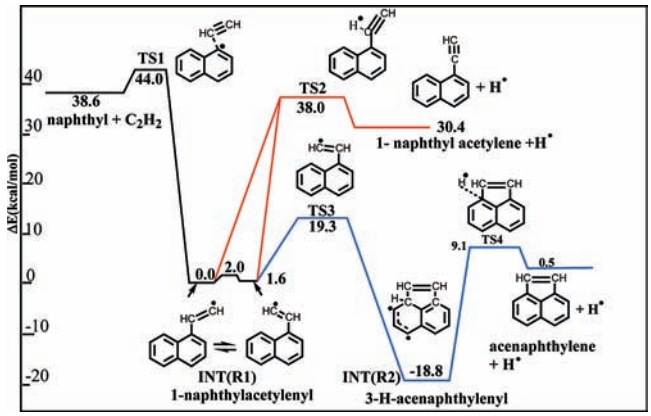

Figure 3. Potential energy surface starting with the reaction: 1-$C_{10}H_7^\bullet$ + C_2H_2 → $C_{10}H_7$−CH═CH$^\bullet$. The surface has two pathways, one producing 1-naphthylacetylene and the other producing acenaphthylene.

of activation, respectively. For the unimolecular reactions, $\Delta H^{\#} = \Delta E^{\#}$, where $\Delta E^{\#}$ is the energy difference between the transition state and the reactant. $\Delta E^{\#}$ is equal to $\Delta E^0_{\text{total}} + \Delta E_{\text{thermal}}$, where $\Delta E^0_{\text{total}}$ is obtained by taking the difference between the total energies of the transition state and the reactant, and $\Delta E_{\text{thermal}}$ is the difference between the thermal energies of these species. In view of relatively low temperatures covered in this investigation and the high size molecules involved, RRKM calculations were not performed.

V. Results of the Quantum Chemical Calculations

The potential energy surface of the 1-naphthyl + acetylene system is shown in Figure 3. The energetics and other parameters relevant to this surface are shown in Table 1. The addition of acetylene to the naphthyl radical toward the formation of a rather stable 1-naphthylacetynyl INT(R1) has a very low barrier of ∼5.5 kcal/mol (TS1). The energy of INT(R1) is taken as zero in both the figure and the table. INT(R1) appears in two isomers that differ from one another in the direction of the $^\bullet$CH═CH− group. The isomerization barrier is ∼2 kcal/mol, so that the two isomers reach equilibrium instantaneously. There are two reaction channels staring from INT(R1). One channel leads to the formation of acenaphthylene, and the second channel leads to the formation of 1-naphthyl acetylene; both involve an H-atom ejection. The bending of the $^\bullet$CH═CH− group toward a five-member ring closure (INT(R2)) proceeds via transition state TS3 with an energy barrier of 19.3 kcal/mol. Only one out of the two INT(R1) isomers can take place in this pathway. This is the isomer where the $^\bullet$CH═CH− group is bent toward the adjacent benzene ring (blue line in Figure 3). This strong bending introduces considerable decrees in entropy (−6.1 cal/(K•mol)) due to its stiff structure. It is accompanied by high exothermicity of 18.8 kcal/mol. The rate-determining step for the formation of acenaphthylene is the H-atom ejection from INT(R2) via transition state TS4 with a barrier of 27.9 kcal/mol.

1-Naphthylacetylene is formed in one step, which is H-atom ejection from INT(R1) via transition state TS2. Both isomers of INT(R1) can participate in this process (red lines in Figure 3). However, the energy barrier of this step is 38 kcal/mol, which is much higher than both the 17.7 kcal/mol for the formation of INT(R2) via transition state TS3 and the 28 kcal/mol that is required to form acenaphthylene via transition state TS4. These differences prevent the production of 1-naphthylacetylene as can be seen in Figures 1 and 2. These results are quite similar to the ones obtained by Richter et al.[1]

VI. Kinetics Scheme and Modeling

1. Reaction Scheme and Results of the Computer Modeling. To compare the single-pulse shock tube experiments to the quantum chemical calculations, a kinetics scheme was constructed and computer modeling was carried out. In addition to the steps that appear on the potential energy surface, the modeling requires several additional steps, such as the production rate of naphthyl radical and some bimolecular reactions involving H-atoms, I-atoms, and other radicals.

The kinetics scheme contains 16 elementary reactions, but only three unimolecular reactions (13−15, Table 2) are based on the potential energy surface of the naphthyl + acetylene system. The rate constant for the unimolecular reaction 16 was taken from our previous 1-naphthylacetylene → acenaphthylene isomerization study.[30] The barriers for reactions 10−12 were calculated by quantum chemical methods in this investigation, but their preexponential factors were estimated on the basis of similar reactions. Reactions 1−9 were either taken from literature sources or were estimated.

The rate constants of reactions 13−15 were obtained from the quantum chemical calculations using eq 1 at several temperatures covering the temperature range 950−1200 K, over which the single-pulse shock tube experiments were carried out. These were then plotted as ln k versus $1/T$ to obtain Arrhenius-

TABLE 1: Total Energies E_{total} (in au), Zero-Point Energies, Relative Energies ΔE,[a] Imaginary Frequencies,[b] and Entropies[c] of the Species in the 1-Naphthyl + C_2H_2 System

	uB3LYP					uCCSD(T)	
species	E_{total}	ΔE^a	ZPE	S^c	ν^b	E_{total}	ΔE^a
1-naphthyl	−385.228877		84.26	83.30		−384.111525	
C_2H_2	−77.333219		15.81	45.19		−77.110121	
1-naphthyl + C_2H_2	−462.562095	39.99	100.07			−461.221646	38.59
TS1	−462.557121	39.17	101.25	104.01	(i − 295)	−461.216467	43.02
INT(R1)	**−462.629472**	**0.0**	**104.36**	**95.35**		**−461.289983**	**0.0**
TS2	−462.561243	37.18	98.73	97.42	(i − 762)	−461.220524	37.96
1-naphthylacetylene + H	−462.567638	32.53	98.09			−461.231582	30.38
1-naphthyl acetylene	−462.066380		98.09	92.18		−460.732304	
TS3	−462.606137	15.73	103.45	89.84	(i − 553)	−461.257780	19.30
INT(R2)	−462.661333	−19.22	105.13	89.25		−461.321129	−18.77
TS4	−462.611069	7.84	100.65	90.16	(i − 851)	−461.269553	9.11
acenaphthylene + H	−462.612949	5.93	99.92			−461.282136	0.48
acenaphthylene	−462.111691		99.92	86.11		−460.782858	

[a] Relative and ZPE energies in kcal/mol. $\Delta E = \Delta E_{\text{total}} + \Delta(\text{ZPE})$. [b] Imaginary frequency in cm^{-1}. [c] Entropies at 298 K in cal/(K•mol).

TABLE 2: 1-Iodonaphthalene−Acetylene Reaction Scheme at 1050 K[a]

no.	reaction	A	$\Delta E^{\#}$	k_f	k_r	ΔS_r	ΔH_r	ref
1	iodonaphthalene → naphthyl$^{\bullet}$ + I$^{\bullet}$	8.59×10^{14}	65.2	23.1	$9.95 \times 10^{+12}$	30.9	64.6	27
2	C_2H_2 + AR → $C_2H^{\bullet}$ + H$^{\bullet}$ + AR	3.88×10^{16}	106.8	2.29×10^{-6}	$9.43 \times 10^{+18}$	33.7	130.0	28
3	C_2H_2 + H$^{\bullet}$→ $C_2H^{\bullet}$ + H_2	9.14×10^{13}	22.9	$1.57 \times 10^{+9}$	$4.79 \times 10^{+12}$	6.5	23.6	28
4	H$^{\bullet}$ + H$^{\bullet}$ + AR → H_2+AR	$8.11 \times 10^{17}T^{-0.81}$	0.16	$2.76 \times 10^{+15}$	2.05×10^{-6}	–27.2	–106.4	28
5	iodonaphthalene + H$^{\bullet}$ → naphthyl$^{\bullet}$ + HI	6.00×10^{13}	6.3	$1.03 \times 10^{+12}$	$6.87 \times 10^{+8}$	6.3	–8.6	est
6	iodonaphthalene + H$^{\bullet}$ → naphthalene + I$^{\bullet}$	3.00×10^{13}	9.4	$1.97 \times 10^{+11}$	58.9	–2.8	–48.8	est
7	H$^{\bullet}$ + I$^{\bullet}$ + AR → HI + AR	$2.00 \times 10^{21}T^{-1.87}$	0	$4.48 \times 10^{+15}$	6.96	–24.6	–73.2	29
8	$C_2H^{\bullet}$ + I$^{\bullet}$ + AR → C_2HI + AR	$2.00 \times 10^{21}T^{-1.87}$	0	$4.48 \times 10^{+15}$	$3.30 \times 10^{+2}$	–32.3	–73.3	29
9	naphthalene → napthyl$^{\bullet}$ + H$^{\bullet}$	5.01×10^{15}	107.9	1.75×10^{-7}	$2.52 \times 10^{+14}$	33.7	113.3	15
10	naphthyl$^{\bullet}$ + H_2 → naphthalene + H$^{\bullet}$	4.00×10^{12}	7.89	$9.13 \times 10^{+10}$	$8.52 \times 10^{+10}$	–6.5	–7.0	*c*
11	naphthyl$^{\bullet}$ + C_2H_2 → INT1(R1)$^{\bullet}$	3.00×10^{12}	5.43	$2.22 \times 10^{+11}$	$1.24 \times 10^{+7}$	–35.3	–33.8	*c*
12	naphthyl$^{\bullet}$ + C_2H_2 → naphthalene + $C_2H^{\bullet}$	3.00×10^{12}	22.0	$7.91 \times 10^{+7}$	$2.26 \times 10^{+11}$	0.03	16.6	*c*
13	INT1(R1)$^{\bullet}$ → 1-naphthylacetylene + H$^{\bullet}$	4.05×10^{14}	41.31	$1.02 \times 10^{+6}$	$2.51 \times 10^{+10}$	30.7	29.6	*b*
14	INT1(R1)$^{\bullet}$ → INT2(R)$^{\bullet}$	1.43×10^{13}	19.46	$1.27 \times 10^{+9}$	$1.77 \times 10^{+6}$	–7.1	–21.2	*b*
15	INT2(R)$^{\bullet}$ → acenaphthylene + H$^{\bullet}$	1.22×10^{14}	30.37	$5.83 \times 10^{+7}$	$1.30 \times 10^{+11}$	27.3	21.1	*b*
16	1-naphthylacetylene → acenaphthylene	3.52×10^{12}	55.9	8.17	1.03×10^{-3}	–10.5	–29.8	30

[a] A factors and rate constants are in cm^3 mol^{-1} s^{-1}; ΔH and $\Delta E^{\#}$ are in kcal/mol, and ΔS is in cal/(K•mol). [b] Obtained from quantum chemical calculations. [c] Barriers from quantum chemical calculations and preexponential factors were estimated.

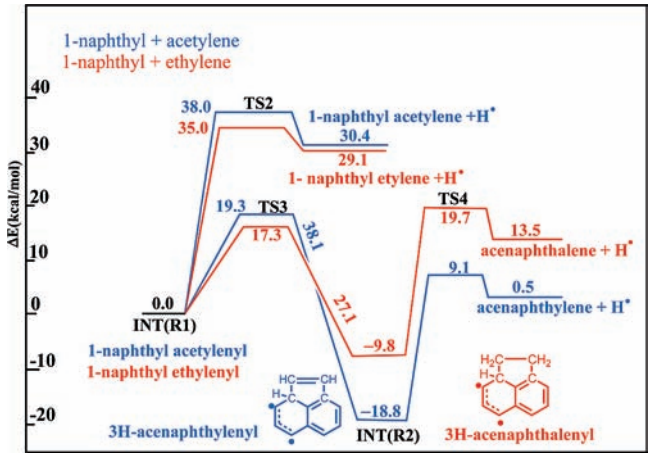

Figure 4. A comparison between the potential energy surfaces of the reactions of naphthyl radicals with acetylene and ethylene. Whereas the surfaces are rather similar, a marked difference, however, is the high barrier for the back reaction of INT(R1) → INT(R2) in acetylene as compared to a considerably lower one in ethylene. This difference explains the production of 1-naphthylaethylene and the absence of 1-naphthylacethylene.

type rate constants that could be used in the modeling. The calculated Arrhenius activation energies and pre-exponential factors are somewhat different from the barriers and the pre-exponential factors that were obtained from the surfaces.

The results of the modeling are shown in Figure 2 as solid lines in comparison with the experimental yields. The + signs on the lines are the calculated points, and the lines are the best fits to these points. As can be seen, the agreement is very good.

VII. Differences and Similarities in the Reaction of 1-Naphthyl Radical with Acetylene and Ethylene

It is of interest to compare the results of the single-pulse shock tube experiments and of the quantum chemical calculations obtained in the reaction of 1-naphthyl radical with acetylene to those that were previously obtained with ethylene. There are two main differences between these two systems. One difference is the formation of 1-naphthyl ethylene (1-vinyl naphthalene) and the absence of the equivalent 1-naphthyl acetylene in the reaction with acetylene. An additional marked difference is the fact that with acetylene the production of acenaphthylene, which is the product of the highest concentration, is the end of the reaction pathway. It does not further decompose or become attacked by H-atoms over the temperature range of the present study. On the other hand, the equivalent product acenaphthalene further reacts with H-atoms to produce acenaphthylene by abstraction reactions.

As can be seen in Figure 4, the two potential energy surfaces starting from INT(R1) (red lines, ethylene; and blue lines, acetylene) are very similar both in the structure of the pathways and energetically, except for one step, which is the back reaction INT(R2) → INT(R1) (via transition state TS3). For ethylene it is ∼27 kcal/mol, whereas for acetylene it is ∼38 kcal/mol. This implies that for acetylene the step INT(R2) → INT(R1) is practically forbidden and the step that produces the acenaphthylene is the only step. The much lower barrier for the INT(R2) → INT(R1) step in ethylene enables this back reaction to take place and to produce 1-naphthyl ethylene. The reason for this different behavior of the two systems is clearly the higher stability of INT(R2) in acetylene. We believe that the delocalization that exists in the latter due to the C═C double bond that does not exist in the ethylene system is the reason for the difference in stabilities.

Acknowledgment. This research was supported by Grant no. 34/01-12.5 from the ISF, The Israel Science Foundation.

References and Notes

(1) Richter, H.; Mazyar, O. A.; Sumathi, R.; Green, W. H.; Howard, J. B.; Bozzelli, J. W. *J. Phys. Chem. A* **2001**, *105*, 1561.
(2) Wang, H.; Frenklach, M. *J. Phys. Chem.* **1994**, *98*, 11465.
(3) Cioslowski, J.; Piskorz, P.; Moncrieff, D. *J. Org. Chem.* **1998**, *63*, 4051.
(4) Violi, A.; Sarofim, A. F.; Truong, T. N. *Combust. Flame* **2001**, *126*, 1506.
(5) Tokmakov, I. V.; Lin, M. C. *J. Am. Chem. Soc.* **2003**, *125*, 11397.
(6) Bockhorn, H.; Fetting, F.; Wenz, H. W. *Ber. Bunsen-Ges. Phys. Chem.* **1983**, *87*, 1067.
(7) Frenklach, M.; Clary, D. W.; Gardiner, W. C.; Stein, S. E. *Proc. Combust. Inst.* **1984**, 2–887.
(8) Frenklach, M.; Warnatz, J. *Combust. Sci. Technol.* **1987**, *51*, 265.
(9) Yu, T.; Lin, M. C.; Melius, C. F. *Int. J. Chem. Kinet.* **1994**, *26*, 1095.
(10) Heckmann, E.; Hippler, H.; Troe, J. *Proc. Combust. Inst.* **1996**, *2*, 6–543.
(11) Tokmakov, I. V.; Lin, M. C. *J. Phys. Chem. A* **2004**, *108*, 9697.
(12) Fahr, A.; Mallard, W. G.; Stein, S. E. *Proc. Combust. Inst.* **1986**, *21*, 825.
(13) Fahr, A.; Stein, S. E. *Proc. Combust. Inst.* **1988**, *22*, 1023.
(14) Yu, T.; Lin, M. C. *Combust. Flame* **1995**, *100*, 169.

(15) Lifshitz, A.; Tamburu, C.; Dubnikova, F. *J. Chem. Phys.* **2008**, *112*, 925.

(16) Lifshitz, A.; Shweky, I.; Kiefer, J. H.; Sidhu, S. S. In *Shock Waves*; Proceedings of the 18th International Symposium on Shock Waves, Sendia, Japan, 1991; Takayama, K., Ed.; Springer-Verlag: Berlin, 1992; p 825.

(17) Tsang, W.; Lifshitz, A. *Int. J. Chem. Kinet.* **1998**, *30*, 621.

(18) Stein, S. E.; Lias, S. G.; Liebman, J. F.; Levin, R. D.; Kafafi, S. A. *NIST Standard Reference Database25, version 2.0*; NIST: Gaithersburg, MD, 1994.

(19) Becke, A. D. *J. Chem. Phys.* **1993**, *98*, 5648.

(20) Lee, C.; Yang, W.; Parr, R. G. *Phys. Rev.* **1988**, *B37*, 785.

(21) Dunning, T. H., Jr. *J. Chem. Phys.* **1989**, *90*, 107.

(22) Peng, C.; Schlegel, H. B. *Isr. J. Chem.* **1993**, *33*, 449.

(23) Pople, J. A.; Head-Gordon, M.; Raghavachari, K. J. *J. Chem. Phys.* **1987**, *87*, 5968.

(24) Frisch, M. J.; Trucks, G. W.; Schlegel, H. B.; Scuseria, G. E.; Robb, M. A.; Cheeseman, J. R.; Montgomery, J. A., Jr.; Vreven, T.; Kudin, K. N.; Burant, J. C.; Millam, J. M.; Iyengar, S. S.; Tomasi, J.; Barone, V.; Mennucci, B.; Cossi, M.; Scalmani, G.; Rega, N.; Petersson, G. A.; Nakatsuji, H.; Hada, M.; Ehara, M.; Toyota, K.; Fukuda, R.; Hasegawa, J.; Ishida, M.; Nakajima, T.; Honda, Y.; Kitao, O.; Nakai, H.; Klene, M.; Li, X.; Knox, J. E.; Hratchian, H. P.; Cross, J. B.; Bakken, V.; Adamo, C.; Jaramillo, J.; Gomperts, R.; Stratmann, R. E.; Yazyev, O.; Austin, A. J.; Cammi, R.; Pomelli, C.; Ochterski, J. W.; Ayala, P. Y.; Morokuma, K.; Voth, G. A.; Salvador, P.; Dannenberg, J. J.; Zakrzewski, V. G.; Dapprich, S.; Daniels, A. D.; Strain, M. C.; Farkas, O.; Malick, D. K.; Rabuck, A. D.; Raghavachari, K.; Foresman, J. B.; Ortiz, J. V.; Cui, Q.; Baboul, A. G.; Clifford, S.; Cioslowski, J.; Stefanov, B. B.; Liu, G.; Liashenko, A.; Piskorz, P.; Komaromi, I.; Martin, R. L.; Fox, D. J.; Keith, T.; Al-Laham, M. A.; Peng, C. Y.; Nanayakkara, A.; Challacombe, M.; Gill, P. M. W.; Johnson, B.; Chen, W.; Wong, M. W.; Gonzalez, C.; Pople, J. A. *Gaussian 03*, revision C.02; Gaussian, Inc.: Wallingford, CT, 2004.

(25) Eyring, H. *J. Chem. Phys.* **1935**, *3*, 107.

(26) Evans, M. G.; Polanyi, M. *Trans. Faraday Soc.* **1935**, *31*, 875.

(27) Robaugh, D.; Tsang, W. *J. Phys. Chem.* **1986**, *90*, 5363.

(28) Westly, F.; Herron, J. T.; Cvetanovic, R. J.; Hampson, R. F.; Mallard, W. G. *NIST-Chemical Kinetics Standard Reference Database17, version 5.0*; NIST: Washington, DC (best fit).

(29) Baulch, D. L.; Duxbury, J.; Grant, S. J.; Montague, D. C. *J. Phys. Chem. Ref. Data* **1981**, *10*, ?????.

(30) Lifshitz, A.; Tamburu, C.; Dubnikova, F. *Proc. Combust. Inst.* **2007**, *31*, 241.

JP905448G